



HHS Public Access

Author manuscript

Brain Behav Immun. Author manuscript; available in PMC 2017 July 01.

Published in final edited form as:

Brain Behav Immun. 2016 July ; 55: 60–69. doi:10.1016/j.bbi.2016.01.006.

Glial Cell Morphological and Density Changes Through the Lifespan of Rhesus Macaques

Katelyn N. Robillard^{1,2}, Kim M. Lee^{1,3}, Kevin B. Chiu¹, and Andrew G. MacLean^{1,3,4,5,*}

¹Tulane National Primate Research Center, Covington, Louisiana

²Southeastern Louisiana University, Hammond, Louisiana

³Tulane Program in Biomedical Sciences, Tulane University School of Medicine, New Orleans, Louisiana

⁴Tulane Program in Neuroscience, Tulane University, New Orleans, Louisiana

⁵Department of Microbiology and Immunology, Tulane University School of Medicine, New Orleans, Louisiana

Abstract

How aging impacts the central nervous system (CNS) is an area of intense interest. Glial morphology is known to affect neuronal and immune function as well as metabolic and homeostatic balance. Activation of glia, both astrocytes and microglia, occurs at several stages during development and aging. The present study analyzed changes in glial morphology and density through the entire lifespan of Rhesus macaques, which are physiologically and anatomically similar to humans. We observed apparent increases in gray matter astrocytic process length and process complexity as rhesus macaques matured from juveniles through adulthood. These changes were not attributed to cell enlargement because they were not accompanied by proportional changes in soma or process volume. There was a decrease in white matter microglial process length as rhesus macaques aged. Aging was shown to have a significant effect on gray matter microglial density, with a significant increase in aged macaques compared with adults. Overall, we observed significant changes in glial morphology as macaques age indicative of astrocytic activation with subsequent increase in microglial density in aged macaques.

Keywords

Aging; glia; astrocyte; microglia

*Corresponding author: Division of Comparative Pathology, Tulane National Primate Research Center, Covington, LA, 70433. amaclean@tulane.edu Telephone: (985) 871 6489.

Publisher's Disclaimer: This is a PDF file of an unedited manuscript that has been accepted for publication. As a service to our customers we are providing this early version of the manuscript. The manuscript will undergo copyediting, typesetting, and review of the resulting proof before it is published in its final citable form. Please note that during the production process errors may be discovered which could affect the content, and all legal disclaimers that apply to the journal pertain.

1 INTRODUCTION

Aging is a normal biological process with changes to numerous physiological functions (see recent review by (Didier et al., 2016) for similarities between primates and humans). Improvements in public health, social services, and healthcare systems worldwide are producing an older human population. Quality of life during aging is dependent upon complex interrelationships between psychosocial and physical health parameters. There are numerous stages in the human and nonhuman primate lifecycle, including infancy, adolescence, adulthood and old-age. Of these, adolescence is noted to be a window of opportunity for “re-wiring” of the nervous system, with reduced spine density on neurons (Spear, 2000). Both astrocytes and microglia are thought to have roles in influencing developmental synaptic pruning (Sofroniew and Vinters, 2010). The purpose of this study was to reveal specific changes in glia during the lifetime of uninfected primates. We chose the prefrontal cortex (PFC) as our region of interest due to its role in higher-order functioning, such as spatial recognition, working memory, and long-term memory. These are impacted during PFC remodeling in adolescence (Spear, 2000) and compromised in age-related neurodegenerative diseases (Czeh et al., 2008).

During normal aging, from juveniles, through adolescence, adulthood and into eugeric aging, the CNS maintains an anti-inflammatory environment, largely through the action of astrocytes (Renner et al., 2011; Yirmiya and Goshen, 2011) and microglia (Ramesh et al., 2013). In these normal conditions, both astrocytes and microglia have a highly ramified morphology, which, for microglia at least, is remarkably consistent across cortical layers (Kongsui et al., 2014). Both astrocytes and microglia assist in glutamatergic signaling, and so structural remodeling of glial processes impacts neuronal signaling (Mayhew et al., 2015). These non-inflammatory roles for glial cells may be part of the normal maturation process (Tremblay, 2011). Indeed, failure of synaptic pruning by microglia induces neurodevelopmental delay (Zhan et al., 2014), and microglial activation *in utero* can have life-long effects (reviewed by Edmonson *et al.*, in press).

Immune cells in the CNS have dual functionalities that can lead to damage of surrounding cells and tissues. Studies have frequently shown a connection between chronic inflammation or stress and the onset of neurodegenerative diseases (Harry, 2013; Hinwood et al., 2013; Middeldorp and Hol, 2011; Orre et al., 2014; Prinz et al., 2011; Tynan et al., 2013). The increase in circulating proinflammatory cytokines in aging humans and nonhuman primates also adversely impacts the CNS. Neural structure and volume are associated with circulating pro-inflammatory cytokines, including IL-6 (Willette et al., 2010), IL-8 and IL-10 (Willette et al., 2013), and combined with increased oxidative stress (Ungvari et al., 2011), indicate a link between chronic inflammation and activation in the CNS.

Microglia are considered the resident macrophages of the brain (Ramesh et al., 2013). These highly ramified cells continuously survey the CNS for abnormalities and may become phagocytic or extend their processes to isolate damaged sites. During infection or injury, microglia can become activated into either a classical (pro-inflammatory) M1 phenotype or alternative (anti-inflammatory) M2 phenotype, depending on signals received from astrocytes and T-cells. Primed microglia can also produce an exaggerated inflammatory

response to a subsequent stimulus (Perry and Holmes, 2014; Renner et al., 2012). The inability of microglia to successfully clear cell debris can induce prolonged inflammation and ultimately lead to depression (Yirmiya et al., 2015), neurodegeneration and premature aging (Harry, 2013; Schwartz et al., 2013).

Because of the close physiological and genetic relationship with humans, studies using nonhuman primates (NHPs) have been invaluable for understanding the changes in brain structure and function that take years, rather than months, to develop (reviewed recently by (Didier et al., 2016)). Thus, the nonhuman primate brain may be an ideal model for eugeric, or normal aging, especially in brain. Rhesus monkeys age approximately 4 times faster than humans (Colman and Anderson, 2011; Kohama et al., 2012; Spear, 2000), providing a unique opportunity to examine glial changes in primates as they age. Importantly, primates are unique in having a distinct adolescent phase of development after puberty, but before true adulthood (Goldman-Rakic, 1987; Spear, 2000; Verrico et al., 2011).

While previous studies have focused on glial activation within one age group or between diseased and controlled states (Lee et al., 2014; Lee et al., 2013a; Lee et al., 2013b; Snook et al., 2013), the present study attempts to identify changes incurred during the entire lifespan in otherwise healthy macaques. Our data will show a sharp increase in the branching, and hence connectivity of glia during the transition from adolescence to adulthood. This occurred concurrently with decreased microglial arbor length. Finally, we noted increased numbers of IBA1 immunopositive cells that were morphologically consistent with microglia in geriatric macaques.

2 MATERIALS AND METHODS

2.1 ETHICS STATEMENT, ANIMAL HOUSING, & SELECTION OF TISSUES

Those animals housed indoors were maintained in Animal Biosafety Level 2 housing with a 12:12- hour light:dark cycle, relative humidity 30% to 70%, and a temperature of 17.8 to 28.9°C. Water was available *ad libitum*, and a standard commercially formulated nonhuman primate diet (Lab Fiber Plus Monkey DT, 5K63, PMI Nutrition International, St. Louis, MO) was provided twice daily and supplemented daily with fresh fruit and/or forage material as part of the environmental enrichment program. All animals at TNPRC have environmental enrichment, widely used to improve welfare in captive macaques. Each cage (Allentown, Inc., Allentown, NJ) measured 36 inches (91.4 centimeters) in height with 8.6 square feet (0.8 square meters) of floor space and contained a perch, a portable enrichment toy, a mirror, and a forage board for feeding enrichment. Practices in the housing and care of animals conformed to the regulations and standards of the U.S. Department of Health and Human Services Public Health Service (PHS) Policy on Humane Care and Use of Laboratory Animals, and the Guide for the Care and Use of Laboratory Animals. The Tulane National Primate Research Center (TNPRC; Animal Welfare Assurance # A4499-01) is fully accredited by the Association for the Assessment and Accreditation of Laboratory Animal Care-International. All animals are routinely cared for according to the guidelines prescribed by the NIH Guide to Laboratory Animal Care. The TNPRC conducts all research in accordance with the recommendations of the Weatherall report - "The use of non-human primates in research". The Institutional Animal Care and Use Committee (IACUC) of the

Tulane National Primate Research Center approved all animal-related protocols, including any treatments used with nonhuman primates. All animal procedures were overseen by veterinarians and their staff.

Animals were humanely euthanized by the veterinary staff at the TNPRC in accordance with endpoint policies. Euthanasia was conducted by anesthesia with ketamine hydrochloride (10 mg/kg) followed by an overdose with sodium pentobarbital and immediate necropsy. This method was consistent with the recommendation of the American Veterinary Medical Association guidelines (Lee et al., 2013b). Three brain regions approximately 1cm thick are routinely collected during necropsy of colony animals at TNPRC representing frontal lobe, parietal & temporal lobe /thalamus/ basal ganglia, and cerebellum / occipital lobe. All tissues are fixed at routine necropsy by immersion in 10% neutral buffered formalin with zinc modification for 48 hours before trimming and paraffin embedding.

The present study stained, imaged, and analyzed formalin fixed paraffin embedded frontal lobe sections collected in the past eight years and stored at the TNPRC tissue archive. All 19 animals constituting this study were uninfected Rhesus macaques that went to necropsy as a result of investigator-initiated control animals, trauma or natural causes. These included 8 males and 11 females ages 0.45 to 25.59 years old (Table 1). Our animals were divided into four groups: juveniles (5 months to 2 years), adolescents (approximately three to five years), adults (seven to twelve years) and geriatrics (twenty years or older) based on general developmental stages (Colman and Anderson, 2011; Kohama et al., 2012; Spear, 2000).

2.2 IMMUNOHISTOCHEMISTRY

Formalin fixed paraffin embedded frontal lobe tissue samples were cut 6 μm thick using an Ultramicrotome. These tissue samples were deparaffinized with Xylene for 25 minutes and rehydrated with decreasing concentrations of ethanol and deionized water. Samples were then incubated in two solutions of Sodium Citrate Buffer: the first solution at room temperature for 30 minutes and the second at >95 degrees for 30 minutes. Tissue samples were allowed to cool in a shaker for 20 minutes before outlined in wax and incubated with DAKO protein block at room temperature for one hour. Next, the protein block was removed, and each sample was incubated overnight at 4°C with 150 μL of a 1:250 dilution of Ionized Calcium-Binding Adaptor Molecule 1 (Iba-1) primary antibody solution (Wako, Richmond, VA). The next day, samples were washed three times in Tris-Buffered Saline (TBS), and each was covered in 150 μL of 1:1000 Alexa 488 Anti-Rabbit secondary antibody. After one hour, the slides were washed three times with TBS and incubated with DAKO block for one hour. After removing the protein block, each sample was incubated for one hour with 150 μL of 1:250 cy-3 pre-conjugated Glial Fibrillary Acidic Protein (GFAP) antibody (clone GA-1, Sigma). Following this, the samples were washed a final three times in TBS. All samples were cover-slipped using Prolong Gold with DAPI and glass slide covers. The slides were refrigerated until imaged by fluorescent microscopy.

The aforementioned Iba-1/GFAP stained slides encompassed all 19 uninfected animals used in this study; these slides were imaged for (1) astrocyte morphology, (2) astrocyte density, and (3) microglia density. A second set of slides including all animals except EB20 was stained only for Iba-1. These slides were imaged for microglia morphological analyses.

2.3 MORPHOMETRIC ANALYSES

Slides were imaged in random order at 40X objective using a Nikon Eclipse TE2000-U microscope. For both astrocytes and microglia, 20 non-overlapping frontal lobe fields were captured for each animal, 10 from gray matter and 10 from white matter. Cells were then analyzed with NeuroLucida software. For astrocyte morphology, 14 cells each from gray (layers 2–6) and white matter were selected at random and traced (Figure 1a). For microglia, 10 cells each from gray (layers 2–6) and white matter were selected and traced (Supplemental Figure 4). For these studies, as with previous studies in this group, only those cells with clear labeling (either GFAP or IBA1) were chosen. It was also important that clear cell bodies were apparent (DAPI staining), and that the processes did not extend beyond the edge of the field imaged. Cells were purposefully chosen far from the gray-white matter border to remain within designated cortical layers, as is routine (Lee et al., 2014; Lee et al., 2013a; Lee et al., 2013b; Snook et al., 2014).

The resulting 2D cell tracings were exported to NeuroLucida Explorer, where morphological characteristics including cell body area, process length, and branch structure analyses were quantitated (Figure 1b, 1c). Using the diameter of the astrocyte processes, frusta were created in NeuroLucida to determine the arbor volume of the astrocyte processes, as is routine (Lee et al., 2014; Lee et al., 2013a; Lee et al., 2013b; Snook et al., 2014). Sholl analyses were also performed in which concentric rings extended from the cell body at 10 μ m increments (Figure 1d). The resulting data were reported per 10 μ m distance from the cell body.

2.4 CONSOLIDATING DATA

Morphological analyses for all animals were imported into Excel and graphed using GraphPad Prism (version 5, GraphPad Software, La Jolla, CA). Branch structure data were assessed for significant changes between age groups using a one-way ANOVA with Bonferroni's Multiple Comparison Test. Sholl data were assessed for significance using a one-way ANOVA with Bonferroni's Multiple Comparison Test. Significant changes between sexes were assessed using an unpaired Student's t-test. For all analyses, significance was defined as $p < 0.05$. Data are presented as mean \pm Standard Deviation.

2.5 CELL DENSITY DETERMINATION

A total of 18 animals were assessed for glial cell density. Five non-overlapping images were captured from both gray and white matter tissue at 20X objective using the Nikon Eclipse TE2000-U microscope. Cells were identified with either IBA1 or GFAP expression and clear cell bodies (DAPI). Each cell was marked using the count feature in Adobe Photoshop CS5 (similar to the count feature in ImageJ), to ensure each cell was counted, but only once. Because most of the imaged gray matter fields included tissue borders, the images were first cropped and the pixel area contained within each field were then converted to μm^2 . The number of each cell type within each tissue area were manually counted and calculated for cell density. Resulting data were analyzed with GraphPad Prism using a one-way ANOVA and Bonferroni's Multiple Comparison Test for significant values ($p < 0.05$).

3. RESULTS

Frontal cortical tissue samples of 19 uninfected macaques were analyzed for age-related changes in glial cell morphology and density throughout the normal primate lifespan. To better assess changes incurred with progressing age, these animals were divided into four distinct groups: (1) juveniles, ages <2 (Figure 1F); (2) adolescence, ages 2–5 (Figure 1E, G); (3) adulthood, ages 7–12 (Figure 1H); (4) and geriatric, ages >18 (Figure 1I). The animals are summarized in Table 1. Animals were also analyzed for morphological changes between sexes.

We postulated that astrocytes would increase in complexity as animals matured. To address this hypothesis, we performed Neurolucida analyses of multiple parameters, as is routine in our laboratory. Kruskal-Wallis analyses showed an effect of age on arbor length of gray matter astrocytes ($p = 0.011$). There was a significant increase in the total arbor length of gray matter astrocytes in adult macaques ($364.3 \pm 83.8\mu\text{m}$) compared to juveniles ($186.1 \pm 41.6\mu\text{m}$; Figure 2A). No significant differences were noted in white matter astrocytes as macaques matured (Figure 2B). Curiously, there were no significant differences observed in apparent arbor volume between any of the groups in either gray or white matter (Supplemental Figure 1 A, B) Thus, we noted that there was a significant increase in arbor length, without a proportional increase in volume. We point out that, GFAP staining to measure complexity may be controversial. If the processes appear to be longer, it is possible that GFAP has accumulated further along the thicker astrocyte processes over time, but the full length of the process may not have changed.

Increased astrocyte size and complexity has been linked to increased cognitive capacity (Han et al., 2013). To determine if the increased length of processes was linked to astrocyte complexity, we calculated the number of nodes and process endpoints (as defined by loss of visible GFAP expression) of each cell. In gray matter astrocytes, there were significant increases in both branching (nodes) and endpoints between adolescents (nodes: 5.8 ± 2.1 , endpoints: 14.9 ± 2.5) and adults (nodes: 15.5 ± 4.2 , endpoints 26.1 ± 5.1). There was also a significant increase in branching between juveniles or adolescents and adults in both gray and white matter astrocytes (Figures 2C and 2D, respectively). The mean number of nodes and endpoints on astrocytes in geriatric animals was significantly less than in adult animals in both gray and white matter.

It is unlikely that these changes were due to inflammatory events, as classically understood, as there was neither hypertrophy nor atrophy of the astrocyte cell bodies (Figure 2E, F). For both gray and white matter astrocytes, there were no significant differences in the number of primary processes between age groups (Supplemental Figure 1 C, D).

In agreement with the data presented in Figure 2A, there was a general increase in length from juveniles to adults at the $20\mu\text{m}$ and $30\mu\text{m}$ marks in gray matter astrocytes when measured using modified Sholl analyses (Figure 3A). The increase in total arbor length is, thus, not attributed to processes extending further from the cell body; rather, the increase represents more branching proximal to the cell body. It is curious that an increase was also observed in white matter astrocytes, with a significant increase from juveniles to adolescents

at the 30 μ m mark (Figure 3B). Thus, as macaques mature from juveniles into adolescence, there are significant increases in apparent complexity and overall arbor length of astrocytes.

We next determined if the increased branching occurred proximally or distally to the astrocyte cell bodies. Thus, we used modified Sholl analyses to investigate changes in process complexity at 10 μ m radial increments from the cell body. This assessment calculated numbers of nodes, ends, intersections (through concentric circles), and length of processes (see Supplemental Figure 2 for details of Sholl analyses of white matter astrocytes). For gray matter astrocytes, there was significantly more branching at the 10 μ m to 30 μ m marks in adult macaques than in any other age group (Figure 3C); this phenomenon was also seen in white matter astrocytes (Figure 3D, and Supplemental Figure 2). There were correspondingly more endpoints in adult macaques at the 20 μ m and 30 μ m marks of both gray and white matter astrocytes (Figures 3E and 3F, respectively). There was a general increase in the number of intersections through Sholl rings from juveniles to adolescents at the 20 μ m and 30 μ m marks (Figure 3G) in gray matter astrocytes. This trend was not observed in white matter astrocytes, which showed no significant changes in numbers of intersections with Sholl rings (Supplemental Figure 2).

When the ages were pooled, there were no significant differences between male (n = 8) and female (n = 11) macaques observed in any of the measured parameters of gray or white matter astrocytes (not shown). The study does not have the potency to find differences between sexes at each age.

To determine if the altered astrocyte morphometrics were correlated with microglial activation, we analyzed microglial remodeling in IBA1 immunopositive cells. Using Kruskal-Wallis analyses, we observed an effect of aging on white matter microglial arbor length. Dunn's post-test analyses showed that there was a decrease in arbor length in white matter microglia in adults ($80.9 \pm 30.6\mu\text{m}$, n = 5) compared to juveniles ($133.8 \pm 5.7\mu\text{m}$, n = 4) (Figure 4D). This is commonly accepted as activation of microglia, with retraction of processes and change to a more amoeboid morphology. However, as with the astrocytes this was not associated with a proportional increase or reduction in process volume or cell body area (Supplemental Figure 3). There was also no significant difference in arbor length in gray matter microglia (Figure 4A), or in the complexity of microglia across the age spectrum in either gray (Figure 4C) or white matter (Figure 4D).

To determine if the decrease in microglial ramification in the adult group was associated with increased microglial migration or proliferation, we determined cell densities by quantifying the number of IBA1-positive cells per mm². There was a significant effect of age on gray matter microglial density [F(3,14) = 3.48, p = 0.045]. Post-hoc comparisons using Tukey's test found that microglia densities in adult rhesus macaques ($122 \text{ cells/mm}^2 \pm 8$) were significantly different from geriatric animals ($189 \text{ cells/mm}^2 \pm 41$) (Figure 5A). A one way between-subjects ANOVA showed a significant effect of age on white matter microglial density [F(3,14) = 3.62, p = 0.040]. However, post-hoc comparisons revealed no significant differences between groups (Figure 5B). For both gray and white matter astrocytes, we found no significant changes in cell density between age groups (gray matter: [F(3,14) =

1.95, $p = 0.17$); white matter: [$F(3,14) = 0.90$, $p = 0.46$]) (Figures 5C and 5D, respectively).

4 DISCUSSION

In the present study, glial cells spanning the age spectrum of rhesus macaques were assessed for changes in morphology and density indicative of CNS inflammation. Atrophy of astrocyte processes has been detected in normal human aging (Heneka et al., 2010), and reversing this atrophy in adult mice improves cognitive abilities (Han et al., 2013). Astrocyte atrophy is also observed in rodent (Tynan et al., 2013) and macaque (Lee et al., 2013b) depression models, resulting in decreased neuronal connectivity and plasticity. Reduced numbers of astrocytes is directly linked to disruptions in cognitive behavior and may be a primary driver of pathology in humans (Banasr and Duman, 2008; Banasr et al., 2011). Our goal was to compare changes in glial morphology and density in normal brains of juvenile, adolescent, adult, and geriatric rhesus macaques.

Astrocytes possess a star-shaped morphology with many branched processes rich in glial fibrillary acidic protein (GFAP) radiating from the cell body, which are more complex in humans and primates compared with rodents and other taxa (Oberheim et al., 2012; Oberheim et al., 2009). In response to injury or infection, astrocytes can respond morphologically via cell body hypertrophy (expansion) and process thickening. This involves altered regulation of actin, tubulin, dynein and Rho pathways (De Filippis et al., 2012; Renner et al., 2013). Activation of these pathways is linked to loss of astrocyte syncytia integrity through downregulation of connexin 43 (Olk et al., 2010). We have recently shown that, even in the absence of continued infectious agent in brain, astrocytes remain activated (Inglis et al., 2015; Lee et al., 2014; Lee et al., 2013a) with regard to morphology and expression of Toll-like Receptor 2 (TLR2) which has been postulated to be a potential driver of glial activation (Snook et al., 2014). Likewise, microglia activation is linked to cytoskeletal alterations, including actin (Uhlemann et al., 2015), to which Iba1 binds. Thus, Iba1 staining is exquisitely sensitive to morphologic changes in microglia (Kongsui et al., 2014; Renner et al., 2012).

In accordance with our original hypothesis, several significant changes were detected in astrocyte morphology between age groups. First, an increase in gray matter astrocytic process length was observed with a concurrent decrease in white matter microglial process length. These changes were not attributed to cell enlargement because they were not accompanied by proportional changes in soma or process volume. The general increase in branching, ends, intersections, and process length on adults compared to all other age groups. Furthermore, this trend was observed only within the first 30 μ m from the cell body. Beyond this, there were no significant differences in any Sholl parameters between age groups (Supplemental Figure 2). Again, these results negate cell enlargement because complexity does not extend further from the cell body as expected with growth. Astrocytic activation in adult macaques and subsequent loss of apparent complexity in geriatrics was in line with the typical onset of neurodegenerative diseases, or age-associated depression (Lalo et al., 2014). We have recently shown a connection between reversible astrocyte atrophy and mood disorders in rhesus macaques (Lee et al., 2015; Lee et al., 2013b).

In the current study, we observed no changes in astrocyte number. The structural atrophy of astrocytes, in the absence of cell loss is associated with depression in other animal models (Tynan et al., 2013). As we observed similar morphometric changes in the geriatric macaques as with animals with symptoms associated with depression (Lee et al., 2013b), it is possible that eugeric aging includes a mild depression associated with astrocyte atrophy (Lalo et al., 2014).

Astrocyte activation in turn could be responsible for, or a result of, microglial activation observed in rhesus macaques (Sloane et al., 1999), although those studies separated geriatrics (over 23) from young adults (between three and ten years of age). Therefore, it is not immediately clear if there was a gradual decline in the previous study. We did observe a gradual decrease in gray matter microglial density from adolescence to adulthood (Figure 5), with the lowest cell density observed in adults. This was followed by a significant increase in grey matter microglial density, in agreement with studies of mouse hippocampus (Giovanoli et al., 2015). This increased neuroinflammation associated with aging will prime the brain to the effects of peripheral infection (Sparkman and Johnson, 2008). It should be noted that all myeloid cells express Iba1, and infiltration of peripheral cells, which is increased during illness and aging, can occur. Additional staining with, e.g. P2RY12 would help to differentiate CNS microglia from peripheral macrophages.

Limitations of this retrospective study of experimentally naïve macaques include the use of 6µm paraffin sections from limited archival tissues. This made truly unbiased stereology impractical without using up the entire tissues from the animals. This is likely to overestimate the cell density especially in those sections containing more cells, and thus, results in a bias because conditions (ages) with higher density are more overestimated than conditions with lower density (Walloe et al., 2014). A further limitation of this study includes underestimation of changes in morphometric parameters using GFAP immunohistochemistry in 6µm paraffin sections. GFAP does not normally stain terminal astrocyte processes. GFAP is a marker of only the astrocytes' cytoskeleton and not its entire volume. There may be other changes in the full volume of the cell that are not observable using GFAP as a marker. GFAP expression to measure volumetric changes may not be consistent with standard practice in the field. However, GFAP staining is routinely used by multiple groups, including ours, to measure changes in astrocyte morphometrics (Braun et al., 2009; Torres-Platas et al., 2015; Tynan et al., 2013). Alternative stains for astrocytes include glutamate transporters (for grey matter), CD44 (for white matter) or prospective Golgi staining (all of which would reveal considerably more astrocyte fine processes than GFAP immunohistochemistry). Combined with thicker sectioning and a motorized Z-stage during analysis, these would capture more astrocytic and microglial processes that were not visible in our 2D fluorescent images. As necropsy is performed on all animals at Tulane National Primate Research Center, a cause of death is assigned to each animal. It is not unexpected that an elderly primate would have some degree of amyloidosis or colitis, as part of the eugeric aging process. As colitis is the first or second most common cause of morbidity in captive rhesus macaques, and there was colitis present in each age group, it is unlikely that idiopathic colitis was linked to any changes in glial activation across the lifespan. We also draw attention to none of the non-geriatric animals having ANY histologic evidence of neuropathology.

Depression has been observed as strong indicators of early-stage dementia and cognitive decline in aging human patients (Leonard, 2007, 2010). Glial morphologic changes, whether microglial (Yirmiya et al., 2015), or astrocytic (Czeh and Di Benedetto, 2013) are common features in models of depression. While this study has revealed the morphological changes incurred by the aging nonhuman primate prefrontal cortex, the origin of these changes has yet to be explained. The current study provides a solid control to which future non-human primate aging studies may be compared. There remain many morphological and physiological changes associated with the uninfected brain that warrant further research.

Supplementary Material

Refer to Web version on PubMed Central for supplementary material.

Acknowledgments

We thank the pathology faculty and staff at Tulane National Primate Research Center for expertly collecting and archiving samples. Ms. Robillard was placed in Dr. MacLean's lab through the efforts of Dr. William Norton, Professor of Biological Sciences, Southeastern Louisiana University, Hammond, Louisiana. This work was supported in part through grants to Dr. MacLean from Tulane University School of Medicine and the Tulane Program in Neuroscience. Ms. Lee was the inaugural TNPRC postgraduate research fellow. PHS grant OD11104, formerly RR00164, were essential for animal husbandry and archiving the tissues for fifty years.

References

- Banasr M, Duman RS. Glial loss in the prefrontal cortex is sufficient to induce depressive-like behaviors. *Biol Psychiatry*. 2008; 64:863–870. [PubMed: 18639237]
- Banasr M, Dwyer JM, Duman RS. Cell atrophy and loss in depression: reversal by antidepressant treatment. *Curr Opin Cell Biol*. 2011; 23:730–737. [PubMed: 21996102]
- Braun K, Antemano R, Helmeke C, Buchner M, Poeggel G. Juvenile separation stress induces rapid region- and layer-specific changes in S100 α - and glial fibrillary acidic protein-immunoreactivity in astrocytes of the rodent medial prefrontal cortex. *Neuroscience*. 2009; 160:629–638. [PubMed: 19285122]
- Colman RJ, Anderson RM. Nonhuman primate calorie restriction. *Antioxid Redox Signal*. 2011; 14:229–239. [PubMed: 20698791]
- Czeh B, Di Benedetto B. Antidepressants act directly on astrocytes: evidences and functional consequences. *Eur Neuropsychopharmacol*. 2013; 23:171–185. [PubMed: 22609317]
- Czeh B, Perez-Cruz C, Fuchs E, Flugge G. Chronic stress-induced cellular changes in the medial prefrontal cortex and their potential clinical implications: does hemisphere location matter? *Behavioural brain research*. 2008; 190:1–13. [PubMed: 18384891]
- De Filippis B, Fabbri A, Simone D, Canese R, Ricceri L, Malchiodi-Albedi F, Laviola G, Fiorentini C. Modulation of RhoGTPases improves the behavioral phenotype and reverses astrocytic deficits in a mouse model of Rett syndrome. *Neuropsychopharmacology*. 2012; 37:1152–1163. [PubMed: 22157810]
- Didier ES, MacLean AG, Mohan M, Didier PJ, Lackner AA, Kuroda MJ. Contributions of Nonhuman Primates to Research on Aging. *Veterinary Pathology*. 2016 in press.
- Giovanoli S, Notter T, Richetto J, Labouesse MA, Vuillermot S, Riva MA, Meyer U. Late prenatal immune activation causes hippocampal deficits in the absence of persistent inflammation across aging. *J Neuroinflammation*. 2015; 12:221. [PubMed: 26602365]
- Goldman-Rakic PS. Development of cortical circuitry and cognitive function. *Child Dev*. 1987; 58:601–622. [PubMed: 3608641]
- Han X, Chen M, Wang F, Windrem M, Wang S, Shanz S, Xu Q, Oberheim NA, Bekar L, Betstadt S, Silva AJ, Takano T, Goldman SA, Nedergaard M. Forebrain engraftment by human glial

- progenitor cells enhances synaptic plasticity and learning in adult mice. *Cell stem cell*. 2013; 12:342–353. [PubMed: 23472873]
- Harry GJ. Microglia during development and aging. *Pharmacol Ther*. 2013; 139:313–326. [PubMed: 23644076]
- Heneka MT, O'Banion MK, Terwel D, Kummer MP. Neuroinflammatory processes in Alzheimer's disease. *J Neural Transm*. 2010; 117:919–947. [PubMed: 20632195]
- Hinwood M, Tynan RJ, Charnley JL, Beynon SB, Day TA, Walker FR. Chronic stress induced remodeling of the prefrontal cortex: structural re-organization of microglia and the inhibitory effect of minocycline. *Cereb Cortex*. 2013; 23:1784–1797. [PubMed: 22710611]
- Inglis FM, Lee KM, Chiu KB, Purcell OM, Didier PJ, Russell-Lodrigue K, Weaver SC, Roy CJ, MacLean AG. Neuropathogenesis of Chikungunya infection: astrogliosis and innate immune activation. *J Neurovirol*. 2015 In Press.
- Kohama SG, Rosene DL, Sherman LS. Age-related changes in human and non-human primate white matter: from myelination disturbances to cognitive decline. *Age*. 2012; 34:1093–1110. [PubMed: 22203458]
- Kongsui R, Beynon SB, Johnson SJ, Walker FR. Quantitative assessment of microglial morphology and density reveals remarkable consistency in the distribution and morphology of cells within the healthy prefrontal cortex of the rat. *J Neuroinflammation*. 2014; 11:182. [PubMed: 25343964]
- Lalo U, Rasooli-Nejad S, Pankratov Y. Exocytosis of gliotransmitters from cortical astrocytes: implications for synaptic plasticity and aging. *Biochem Soc Trans*. 2014; 42:1275–1281. [PubMed: 25233403]
- Lee KM, Chiu KB, Didier PJ, Baker KC, MacLean AG. Naltrexone treatment reverses astrocyte atrophy and immune dysfunction in self-harming macaques. *Brain Behav Immun*. 2015
- Lee KM, Chiu KB, Renner NA, Sansing HA, Didier PJ, MacLean AG. Form follows function: astrocyte morphology and immune dysfunction in SIV neuroAIDS. *J Neurovirol*. 2014; 20:474–484. [PubMed: 24970236]
- Lee KM, Chiu KB, Sansing HA, Didier PJ, Ficht TA, Arenas-Gamboa AM, Roy CJ, Maclean AG. Aerosol-induced brucellosis increases TLR-2 expression and increased complexity in the microanatomy of astroglia in rhesus macaques. *Frontiers in cellular and infection microbiology*. 2013a; 3:86. [PubMed: 24350061]
- Lee KM, Chiu KB, Sansing HA, Inglis FM, Baker KC, Maclean AG. Astrocyte atrophy and immune dysfunction in self-harming macaques. *PLoS One*. 2013b; 8:e69980. [PubMed: 23922882]
- Leonard BE. Inflammation, depression and dementia: are they connected? *Neurochemical research*. 2007; 32:1749–1756. [PubMed: 17705097]
- Leonard BE. The concept of depression as a dysfunction of the immune system. *Curr Immunol Rev*. 2010; 6:205–212. [PubMed: 21170282]
- Mayhew J, Beart PM, Walker FR. Astrocyte and microglial control of glutamatergic signalling: a primer on understanding the disruptive role of chronic stress. *J Neuroendocrinol*. 2015; 27:498–506. [PubMed: 25737228]
- Middeldorp J, Hol EM. GFAP in health and disease. *Prog Neurobiol*. 2011; 93:421–443. [PubMed: 21219963]
- Oberheim NA, Goldman SA, Nedergaard M. Heterogeneity of astrocytic form and function. *Methods Mol Biol*. 2012; 814:23–45. [PubMed: 22144298]
- Oberheim NA, Takano T, Han X, He W, Lin JH, Wang F, Xu Q, Wyatt JD, Pilcher W, Ojemann JG, Ransom BR, Goldman SA, Nedergaard M. Uniquely hominid features of adult human astrocytes. *The Journal of neuroscience: the official journal of the Society for Neuroscience*. 2009; 29:3276–3287. [PubMed: 19279265]
- Olk S, Turchinovich A, Grzendowski M, Stuhler K, Meyer HE, Zoidl G, Dermietzel R. Proteomic analysis of astroglial connexin43 silencing uncovers a cytoskeletal platform involved in process formation and migration. *Glia*. 2010; 58:494–505. [PubMed: 19795503]
- Orre M, Kamphuis W, Osborn LM, Jansen AH, Kooijman L, Bossers K, Hol EM. Isolation of glia from Alzheimer's mice reveals inflammation and dysfunction. *Neurobiol Aging*. 2014; 35:2746–2760. [PubMed: 25002035]

- Perry VH, Holmes C. Microglial priming in neurodegenerative disease. *Nature reviews Neurology*. 2014; 10:217–224. [PubMed: 24638131]
- Prinz M, Priller J, Sisodia SS, Ransohoff RM. Heterogeneity of CNS myeloid cells and their roles in neurodegeneration. *Nature neuroscience*. 2011; 14:1227–1235. [PubMed: 21952260]
- Ramesh G, Maclean AG, Philipp MT. Cytokines and Chemokines at the Crossroads of Neuroinflammation, Neurodegeneration, and Neuropathic Pain. *Mediators Inflamm*. 2013; 2013:480739. [PubMed: 23997430]
- Renner, NA.; Lackner, AA.; MacLean, AG. Blood-Brain Barrier Disruption and Encephalitis in Animal Models of AIDS. In: Tkachev, S., editor. *Non-Flavivirus Encephalitis*. In Tech; 2011. p. 87-102.
- Renner NA, Sansing HA, Inglis FM, Mehra S, Kaushal D, Lackner AA, Maclean AG. Transient acidification and subsequent proinflammatory cytokine stimulation of astrocytes induce distinct activation phenotypes. *J Cell Physiol*. 2013; 228:1284–1294. [PubMed: 23154943]
- Renner NA, Sansing HA, Morici LA, Inglis FM, Lackner AA, Maclean AG. Microglia activation by SIV-infected macrophages: alterations in morphology and cytokine secretion. *J Neurovirol*. 2012; 18:213–221. [PubMed: 22535448]
- Schwartz M, Kipnis J, Rivest S, Prat A. How do immune cells support and shape the brain in health, disease, and aging? *J Neurosci*. 2013; 33:17587–17596. [PubMed: 24198349]
- Sloane JA, Hollander W, Moss MB, Rosene DL, Abraham CR. Increased microglial activation and protein nitration in white matter of the aging monkey. *Neurobiol Aging*. 1999; 20:395–405. [PubMed: 10604432]
- Snook ER, Fisher-Perkins JM, Sansing HA, Lee KM, Alvarez X, Maclean AG, Peterson KE, Lackner AA, Bunnell BA. Innate Immune Activation in the Pathogenesis of a Murine Model of Globoid Cell Leukodystrophy. *Am J Pathol*. 2013
- Snook ER, Fisher-Perkins JM, Sansing HA, Lee KM, Alvarez X, MacLean AG, Peterson KE, Lackner AA, Bunnell BA. Innate immune activation in the pathogenesis of a murine model of globoid cell leukodystrophy. *Am J Pathol*. 2014; 184:382–396. [PubMed: 24316110]
- Sofroniew MV, Vinters HV. Astrocytes: biology and pathology. *Acta Neuropathol*. 2010; 119:7–35. [PubMed: 20012068]
- Sparkman NL, Johnson RW. Neuroinflammation associated with aging sensitizes the brain to the effects of infection or stress. *Neuroimmunomodulation*. 2008; 15:323–330. [PubMed: 19047808]
- Spear LP. The adolescent brain and age-related behavioral manifestations. *Neurosci Biobehav Rev*. 2000; 24:417–463. [PubMed: 10817843]
- Torres-Platas SG, Nagy C, Wakid M, Turecki G, Mechawar N. Glial fibrillary acidic protein is differentially expressed across cortical and subcortical regions in healthy brains and downregulated in the thalamus and caudate nucleus of depressed suicides. *Mol Psychiatry*. 2015
- Tremblay ME. The role of microglia at synapses in the healthy CNS: novel insights from recent imaging studies. *Neuron Glia Biol*. 2011; 7:67–76. [PubMed: 22418067]
- Tynan RJ, Beynon SB, Hinwood M, Johnson SJ, Nilsson M, Woods JJ, Walker FR. Chronic stress-induced disruption of the astrocyte network is driven by structural atrophy and not loss of astrocytes. *Acta Neuropathol*. 2013; 126:75–91. [PubMed: 23512378]
- Uhlemann R, Gertz K, Boehmerle W, Schwarz T, Nolte C, Freyer D, Kettenmann H, Endres M, Kronenberg G. Actin dynamics shape microglia effector functions. *Brain structure & function*. 2015
- Ungvari Z, Bailey-Downs L, Gautam T, Sosnowska D, Wang M, Monticone RE, Telljohann R, Pinto JT, de Cabo R, Sonntag WE, Lakatta EG, Csiszar A. Age-associated vascular oxidative stress, Nrf2 dysfunction, and NF- κ B activation in the nonhuman primate *Macaca mulatta*. *The journals of gerontology Series A, Biological sciences and medical sciences*. 2011; 66:866–875.
- Verrico CD, Liu S, Asafu-Adjei JK, Sampson AR, Bradberry CW, Lewis DA. Acquisition and baseline performance of working memory tasks by adolescent rhesus monkeys. *Brain Res*. 2011; 1378:91–104. [PubMed: 21215729]
- Walloe S, Pakkenberg B, Fabricius K. Stereological estimation of total cell numbers in the human cerebral and cerebellar cortex. *Frontiers in human neuroscience*. 2014; 8:508. [PubMed: 25076882]

- Willette AA, Bendlin BB, McLaren DG, Canu E, Kastman EK, Kosmatka KJ, Xu G, Field AS, Alexander AL, Colman RJ, Weindruch RH, Coe CL, Johnson SC. Age-related changes in neural volume and microstructure associated with interleukin-6 are ameliorated by a calorie-restricted diet in old rhesus monkeys. *NeuroImage*. 2010; 51:987–994. [PubMed: 20298794]
- Willette AA, Coe CL, Birdsill AC, Bendlin BB, Colman RJ, Alexander AL, Allison DB, Weindruch RH, Johnson SC. Interleukin-8 and interleukin-10, brain volume and microstructure, and the influence of calorie restriction in old rhesus macaques. *Age*. 2013; 35:2215–2227. [PubMed: 23463321]
- Yirmiya R, Goshen I. Immune modulation of learning, memory, neural plasticity and neurogenesis. *Brain Behav Immun*. 2011; 25:181–213. [PubMed: 20970492]
- Yirmiya R, Rimmerman N, Reshef R. Depression as a Microglial Disease. *Trends Neurosci*. 2015; 38:637–658. [PubMed: 26442697]
- Zhan Y, Paolicelli RC, Sforzini F, Weinhard L, Bolasco G, Pagani F, Vyssotski AL, Bifone A, Gozzi A, Ragozzino D, Gross CT. Deficient neuron-microglia signaling results in impaired functional brain connectivity and social behavior. *Nat Neurosci*. 2014; 17:400–406. [PubMed: 24487234]

Highlights

Astrocytes become more complex during aging, peaking in adulthood

Most complexity increase occurs close to astrocyte cell body

Microglia become less complex, indicating possible activation

Depression in eugenic aging could have a glial component

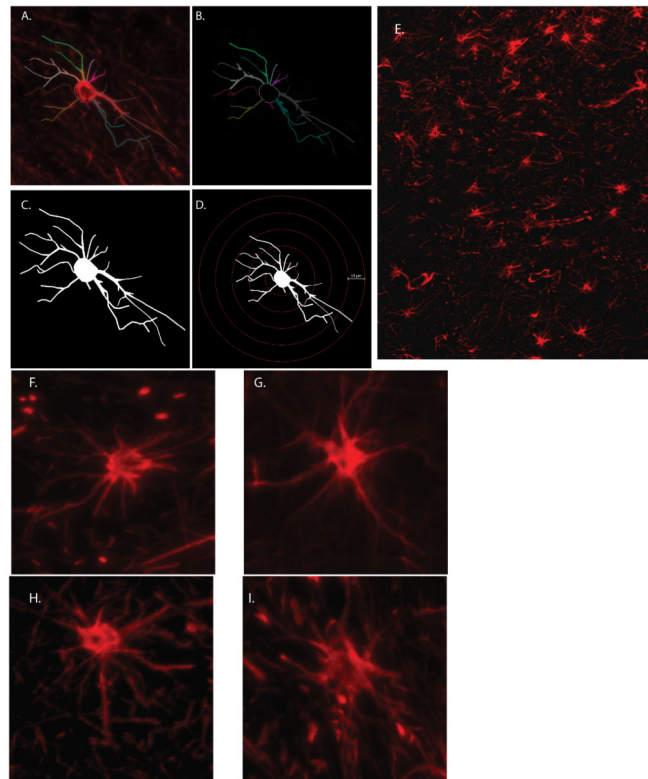


Figure 1. Determination of Cell Morphology

GFAP-stained astrocytes (red) were imaged by fluorescent microscopy at 40x objective (A), and then traced with Neurolucida software (B), which assigns arbitrary colors to the cell processes. Cells were then analyzed for branch structure parameters (C), and then a modified Sholl analysis was performed (D). GFAP-immunopositive astrocytes were first identified at low power (10x, E., white matter of adolescent macaque), and those cells that did not touch the edges of fields were imaged at 40x (Juvenile, F, Adolescent, G, Adult H, and geriatric I).

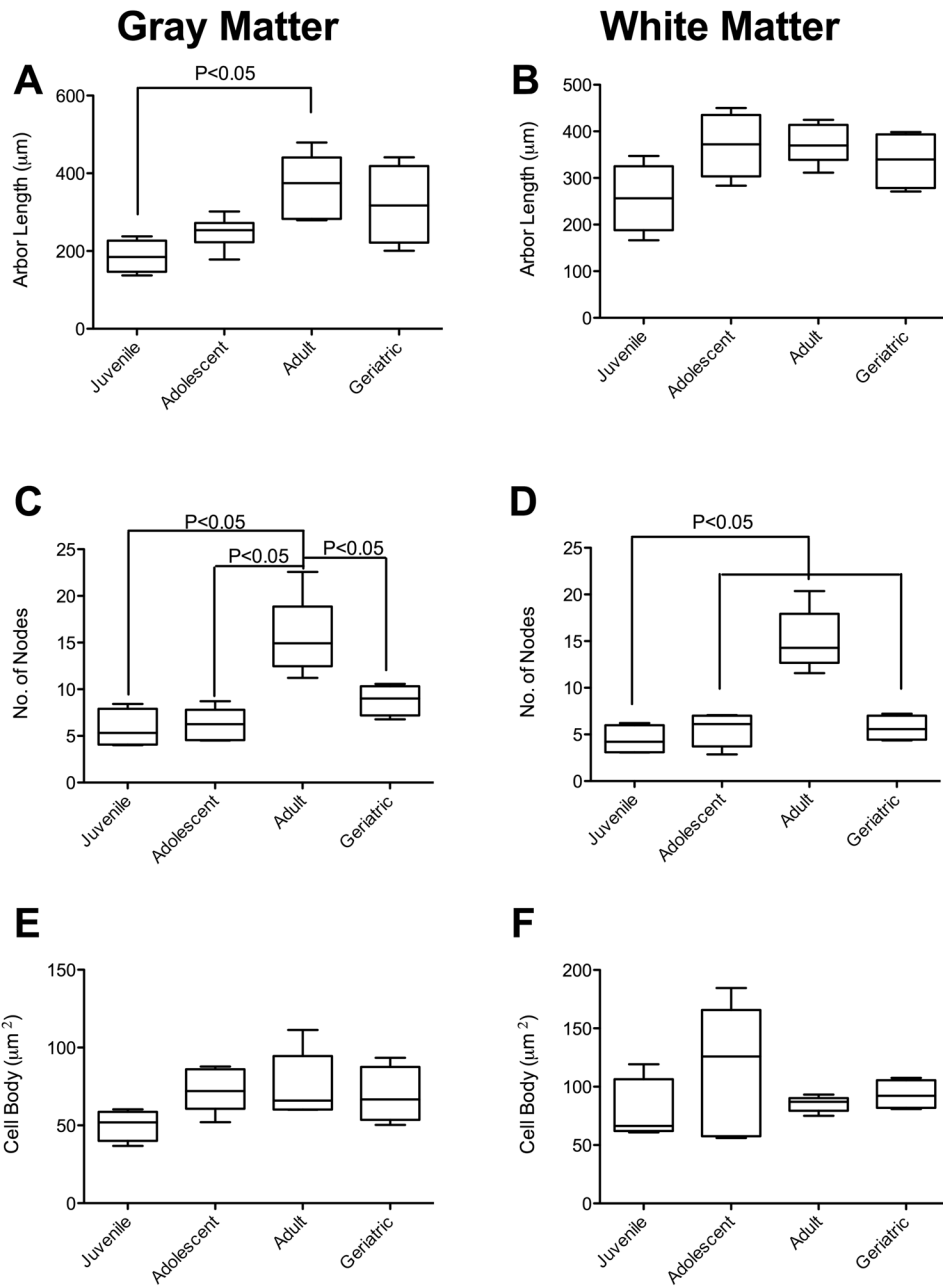


Figure 2. Age-associated Morphologic Changes in Primate Astrocytes

A general increase in total process length of gray matter astrocytes was observed, with significant increase between juveniles and adults (A). There was no significant increase in white matter process length as macaques matured (B). The apparent complexity of the astrocytes was significantly increased in both gray (C) and white matter (D) astrocytes as macaques became adults, which was then decreased in geriatrics. These changes were not associated with either atrophy or hypertrophy in either gray (E) or white matter (F) cell bodies.

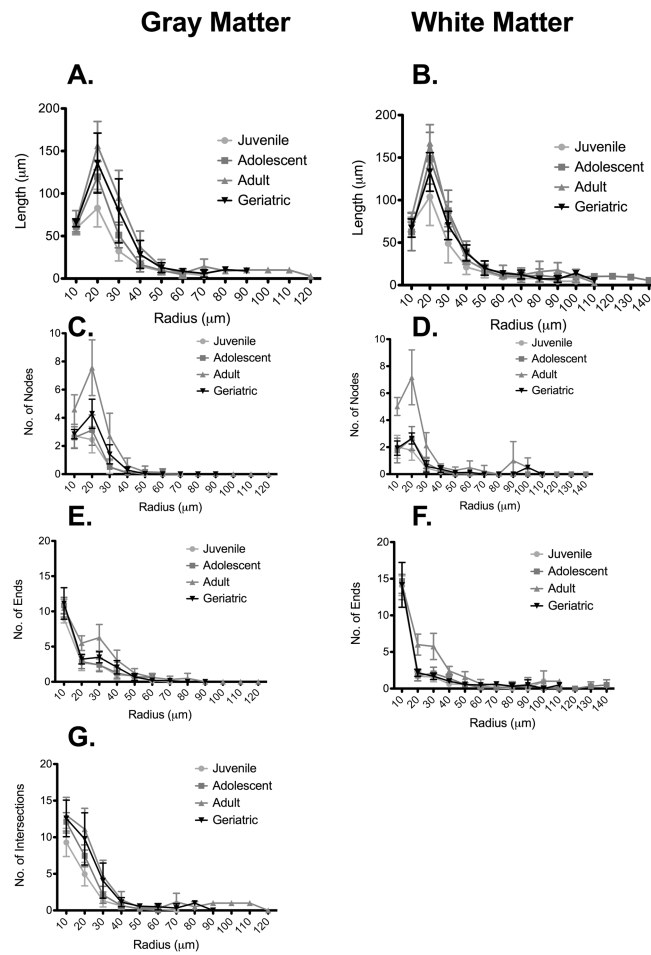


Figure 3. Astrocyte complexity occurs proximally rather than distally
Sholl analyses showed that, compared with other age groups, adult macaques had increases in length (A, B), and nodes (C,D) within the first 30 μm of the cell processes in both gray and white matter. It was interesting that there were also increased number of endings (E, F) within the first 30 μm , indicating numerous short processes in the adult astrocytes, absent from other age groups. The number of intersections in gray matter was also increased in adults (G).

Gray Matter

White Matter

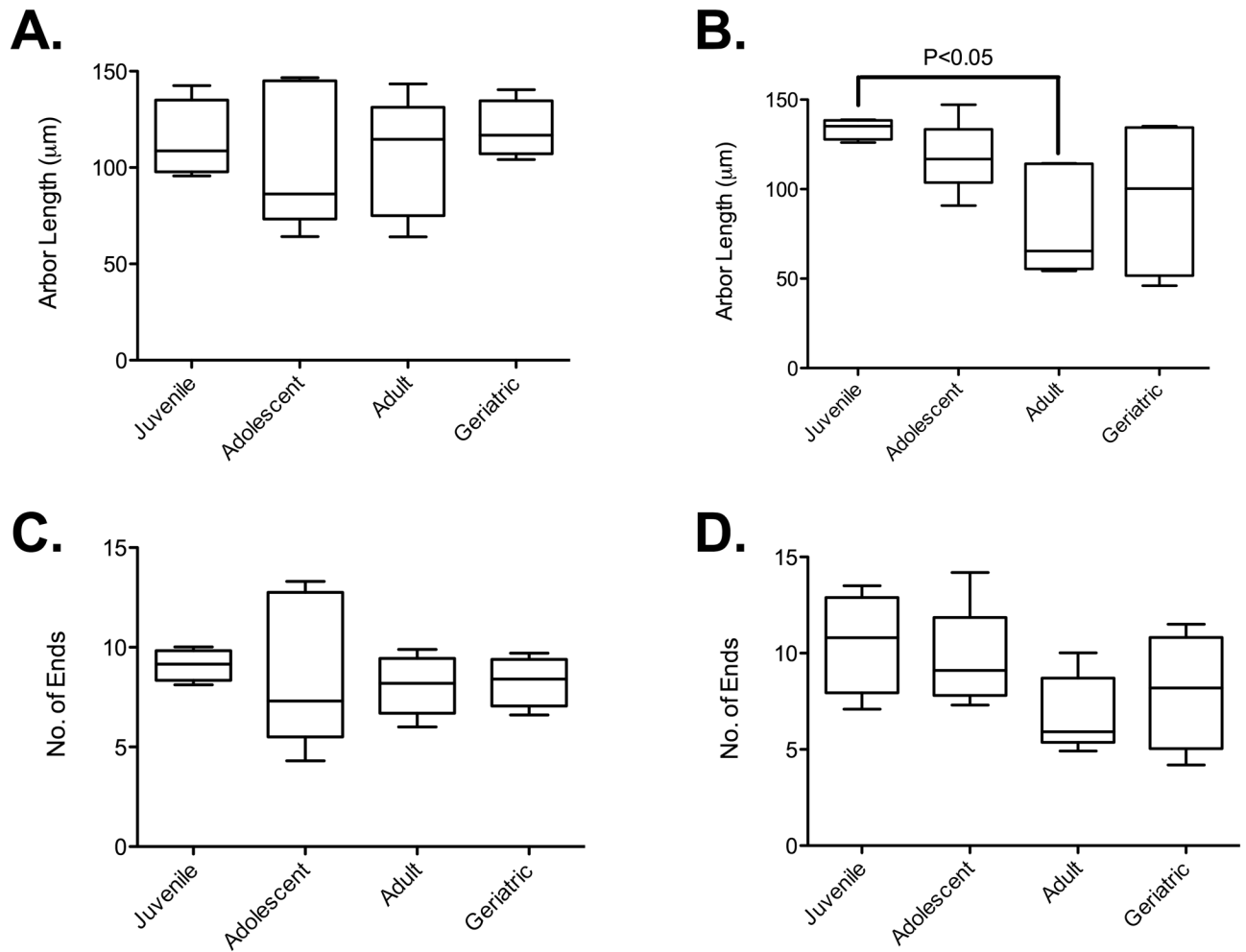


Figure 4. Age-associated Morphologic Changes in Primate Microglia

There was no significant change in the arbor length of gray matter microglia across the age spectrum (A). There was a significantly reduced arbor, however, in white matter between juvenile microglia and those in adult macaques (B). There was no significant alteration in the complexity of the microglia in either gray (C) or white matter (D) across the age spectrum examined.

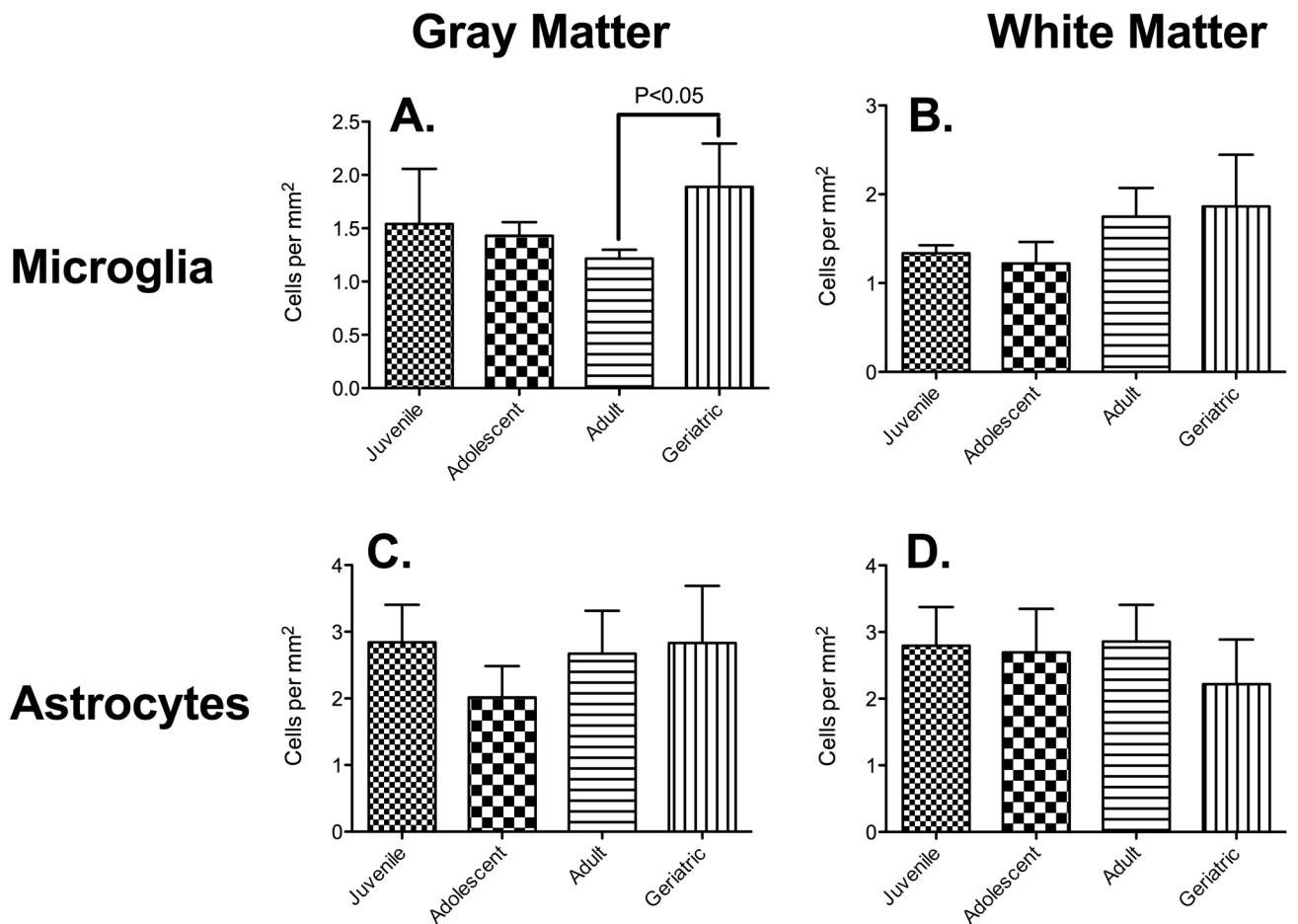


Figure 5. Increased Numbers of Microglia but not Astrocytes in Geriatric Primates

There was a significant increase in the number of microglia in gray matter as macaques matured from adults into geriatrics (A). The increase in microglia cell density in white matter from adolescents to geriatrics was not significant, however (B). There was no significant change in astrocyte density in either gray (C) or white matter (D).

Table 1

Animals, age groups, genders and neuropathologic findings

	ANIMAL	AGE	SEX	NEUROPATHOLOGIC FINDINGS	FINAL CAUSE OF DEATH
Juveniles	IG30	0.45	F	NONE	COLITIS
	HN83	0.77	F	NONE	COLITIS
	IL06**	1.37	M	NONE	COLITIS
	IK77	1.84	F	NONE	COLITIS
Adolescents	HT22	2.91	M	NONE	INVESTIGATOR-INITIATED FOR CONTROL TISSUES
	HP24	3.03	M	NONE	INVESTIGATOR-INITIATED FOR CONTROL TISSUES
	HN64	3.03	M	NONE	INVESTIGATOR-INITIATED FOR CONTROL TISSUES
	HM63	3.04	M	NONE	INVESTIGATOR-INITIATED FOR CONTROL TISSUES
	EB20*	3.82	F	NONE	COLITIS
	EI93	5.31	F	NONE	INTESTINAL AMYLOIDOSIS
	FL13	7.18	M	NONE	COLITIS
Adults	F138	7.60	F	NONE	ARTHRITIS (KNEES)
	FD65	7.8	F	NONE	YEAST INFECTION (LUNGS)
	DE83	10.17	M	NONE	INTESTINAL AMYLOIDOSIS
	CT65	12.45	F	NONE	COLITIS
	N142	18.98	M	LIPODYSTROPHY (CEREBRUM)	GENERALIZED AMYLOIDOSIS
Geriatrics	IR85	20.49	F	NONE	COLITIS
	I730	22.43	F	LIPOFUSCINOSIS ASSOCIATED WITH AGING, BRAIN STEM DEGENERATION	TRAUMA/MONKEY BITE
	F470	25.59	F	NONE	GENERALIZED AMYLOIDOSIS